Electronic Supplementary Material (ESI) for Journal of Materials Chemistry A.

Accelerated Identification of High-Performance Catalysts for Low-Temperature NH_3-SCR by Machine Learning

Yi Dong, Yu Zhang, Mingchu Ran, Xiao Zhang*, Shaojun Liu,Yang Yang, Wenshuo Hu, Chenghang Zheng, Xiang Gao*

State Key Laboratory of Clean Energy Utilization, State Environmental Protection Center for Coal-Fired Air Pollution Control, Zhejiang University, 38 Zheda Road, Hangzhou, 310027, China

Corresponding author. Tel.: +86 571 87951335
E-mail address: xgao1@zju.edu.cn (X. Gao); zhangx_energy@zju.edu.cn (X. Zhang)

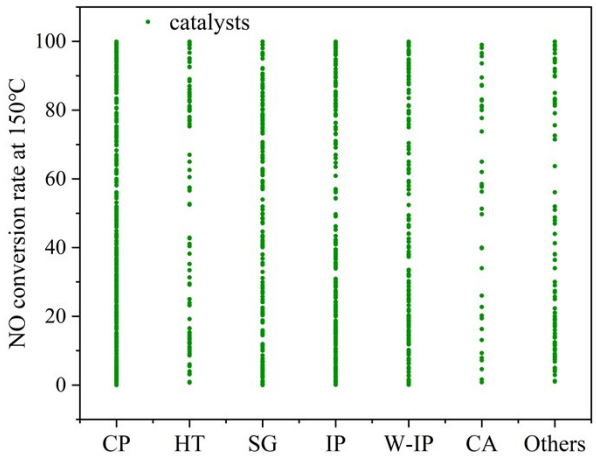

Fig. S1. The activity distribution diagram of catalysts prepared by different methods. CP: co-precipitation, HT: Hydrothermal method, SG: sol-gel, IP: impregnation, W-IP: wet incipient impregnation, CA: citric acid.

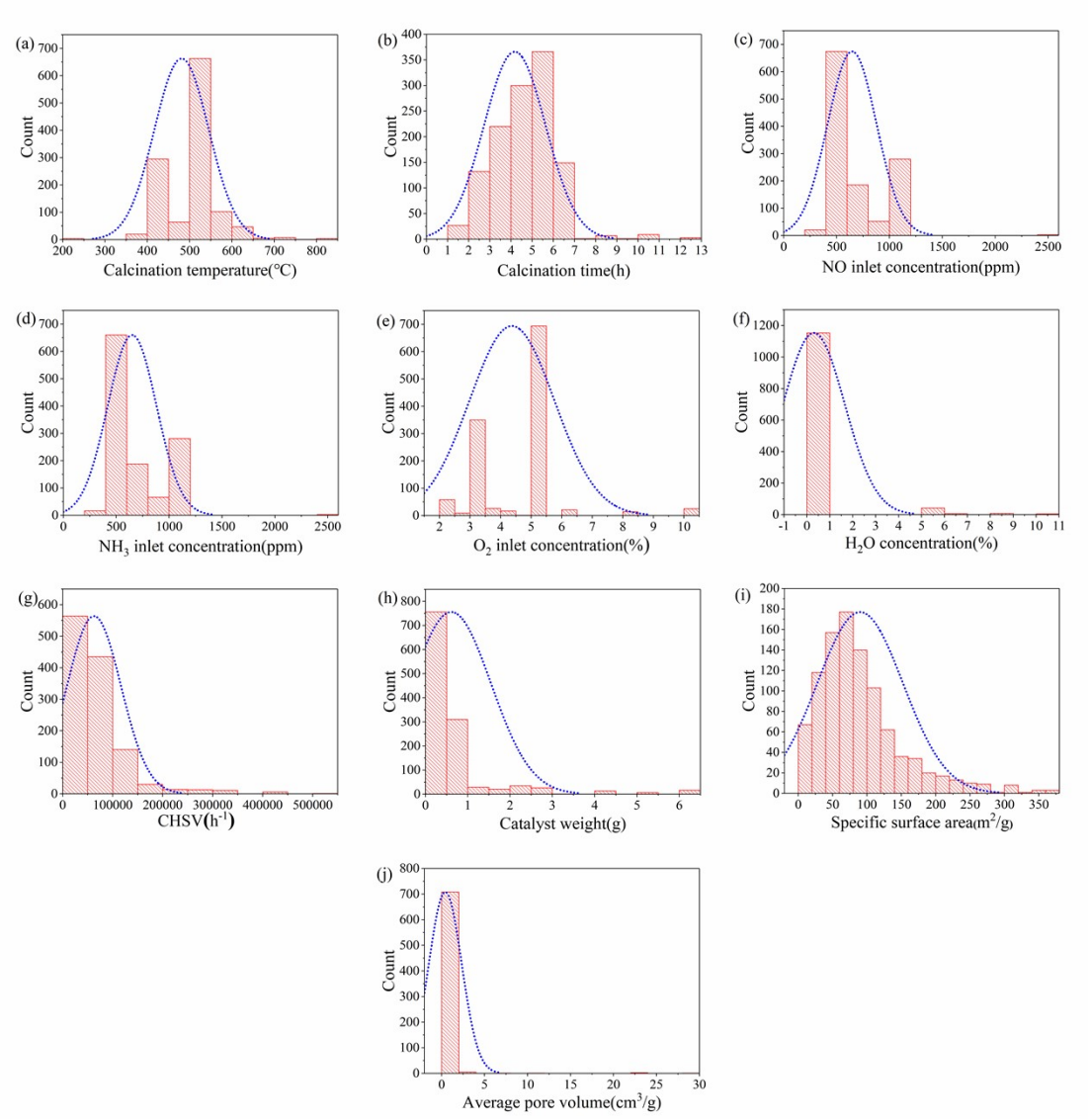

Fig. S2. Histogram of the the input data layers of (a) Calcination temperature, (b) Calcination time, (c) NO inlet concentration, (d) NH_3 inlet concentration, (e) O_2 inlet concentration, (f) H_2O inlet concentration, (h) catalyst weight, (i) specific surface area, (j) average pore volume, the blue dashed line is the normal distribution curve.

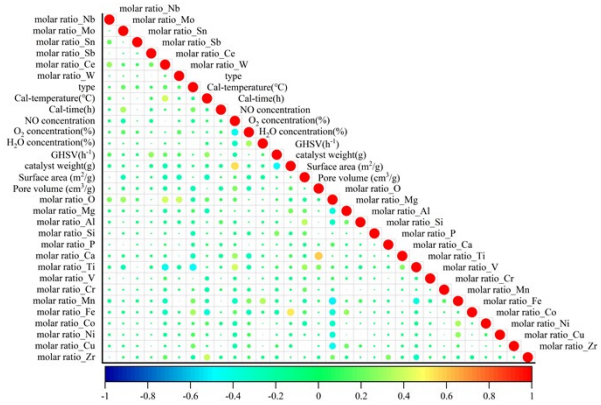

Fig. S3. The correlation heat map for the individual primary features with themselves in the dataset.

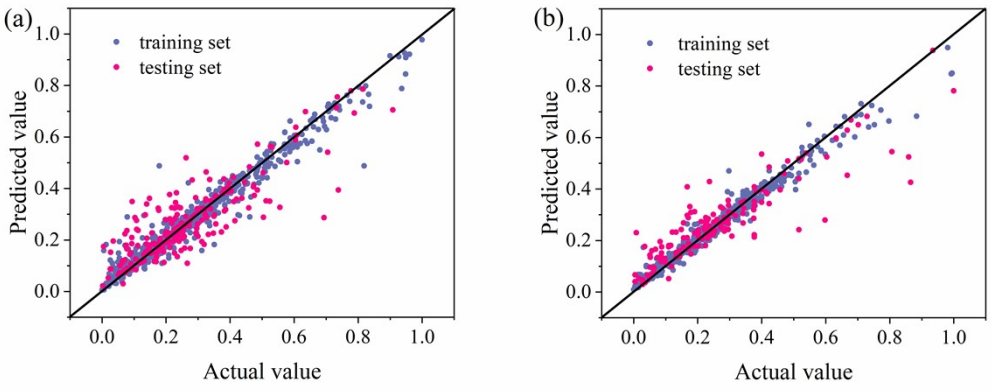

Fig. S4. The comparison of actual and predicted values of the regression model for predicting (a) specific surface area, (b) average pore diameter: blue dot: training set, red dot: testing set.

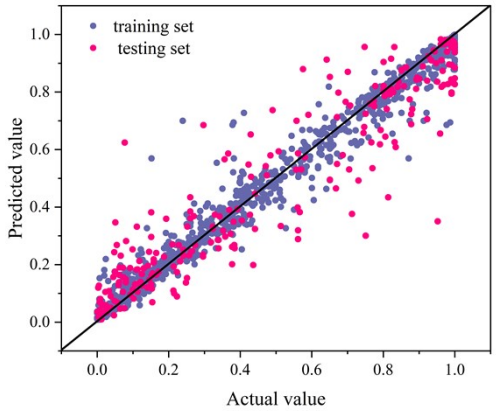

Fig. S5. The comparison of actual and predicted values of the Pattern D: using the feature vector does not include specific surface area and average pore volume, blue dot: training set, red dot: testing set.

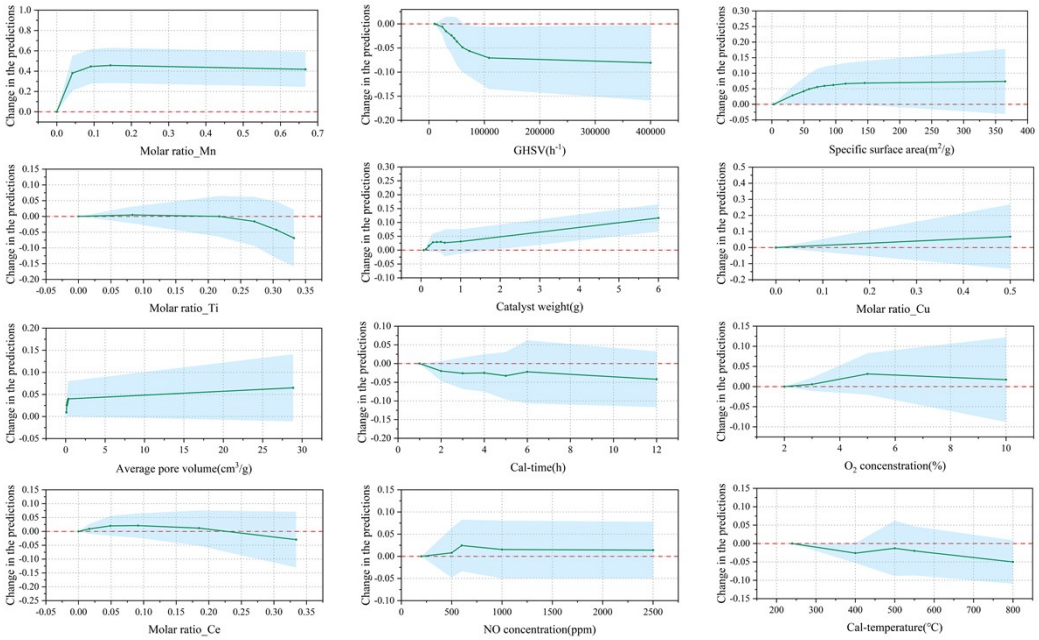

Fig. S6. Partial dependence plot for twelve most important variables (The blue shaded part indicates the confidence interval).

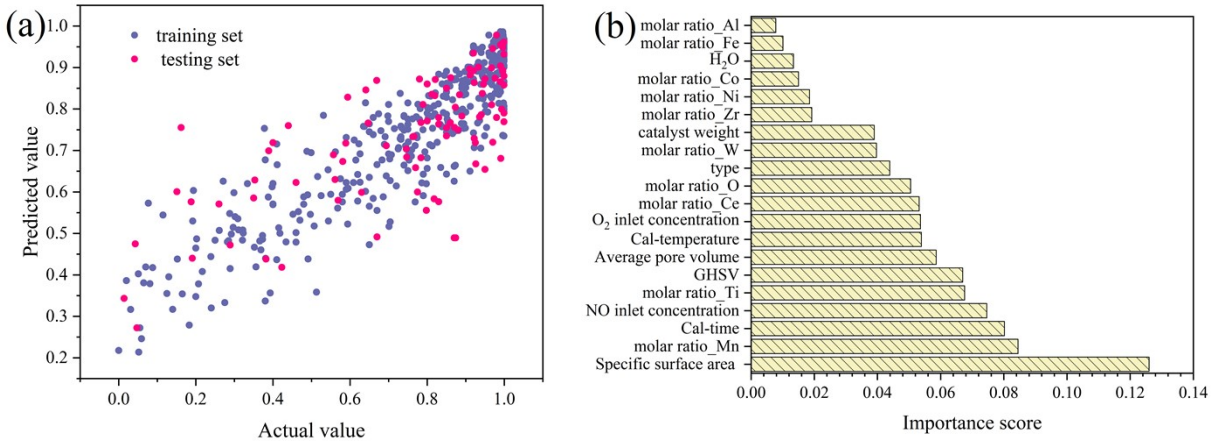

Fig. S7. (a)The comparison of actual and predicted values for the training sets and testing sets: Pattern E (b) The importance score of the top 20 features.

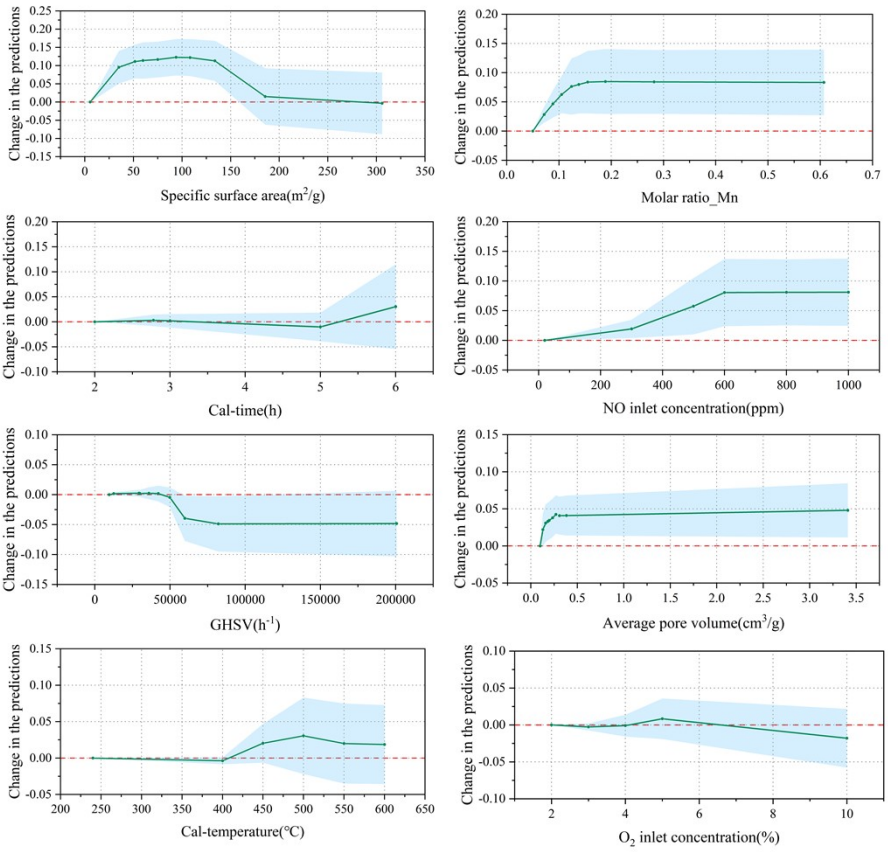

Fig. S8. Partial dependence plot for twelve most important variables (The blue shaded part indicates the confidence interval).

X-ray diffraction (XRD) patterns were measured by a PANalytical X'Pert PRO XRD system, which was equipped with a Cu Kα radiation in the 2θ range from 10° to 80° and a scanning rate of 4° min^{-1}.N_2 adsorption and desorption experiments were carried out at liquid nitrogen temperature (−196 °C) over a range of relative pressures using an ASAP 2460 (Micromeritics Instrument Crop.), after being outgassed at 300 °C for 4 h. The specific area was computed using the Brunauer-Emmett-Teller (BET) method, while pore size distribution and average pore diameter were calculated by Barrett-Joyner-Halenda (BJH) method. SEM–EDS was performed with SU-8010 (Hitachi, Ltd., Tokyo, Japan).

Fig. S9 represented the XRD patterns of the Mn-Ce-M (M=Co, Fe, Cu) catalysts. For Mn-Ce-Co catalyst, it presented sharp peaks at 2θ = 19°, 36.7°, 44.8°, 59.3°, 65.2°, which belong to (111), (311), (400), (511), (440) planes of Co_3O_4 (PDF#80-1532), while the diffraction peaks of CeO_2, MnO_2 were not detected. For Mn-Ce-Fe catalyst,

serval sharp peaks presented at 2θ = 28.9°, 36.1°, 59.9° belong to (112), (211), (224) planes of Mn_3O_4 (PDF#75-1560), 2θ = 47.4°, 56.3° belong to (220), (311) planes of CeO_2 (PDF#81-0792), while the diffraction peaks of Fe_2O_3 were not detected. For Mn-Ce-Cu catalyst, serval sharp peaks presented at 2θ = 28.5°, 33°, 47.4°, 56.3°belong to (111), (220), (222), (311) planes of CeO_2 (PDF#81-0792), 2θ = 28.9° belong to (112) plane of Mn_3O_4 (PDF#75-1560), while the diffraction peaks of CuO were not detected.

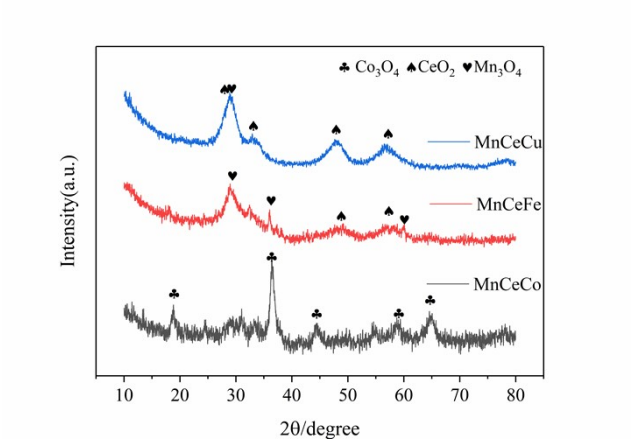

Fig. S9. XRD patterns of Mn-Ce-M (M=Co, Fe, Cu).

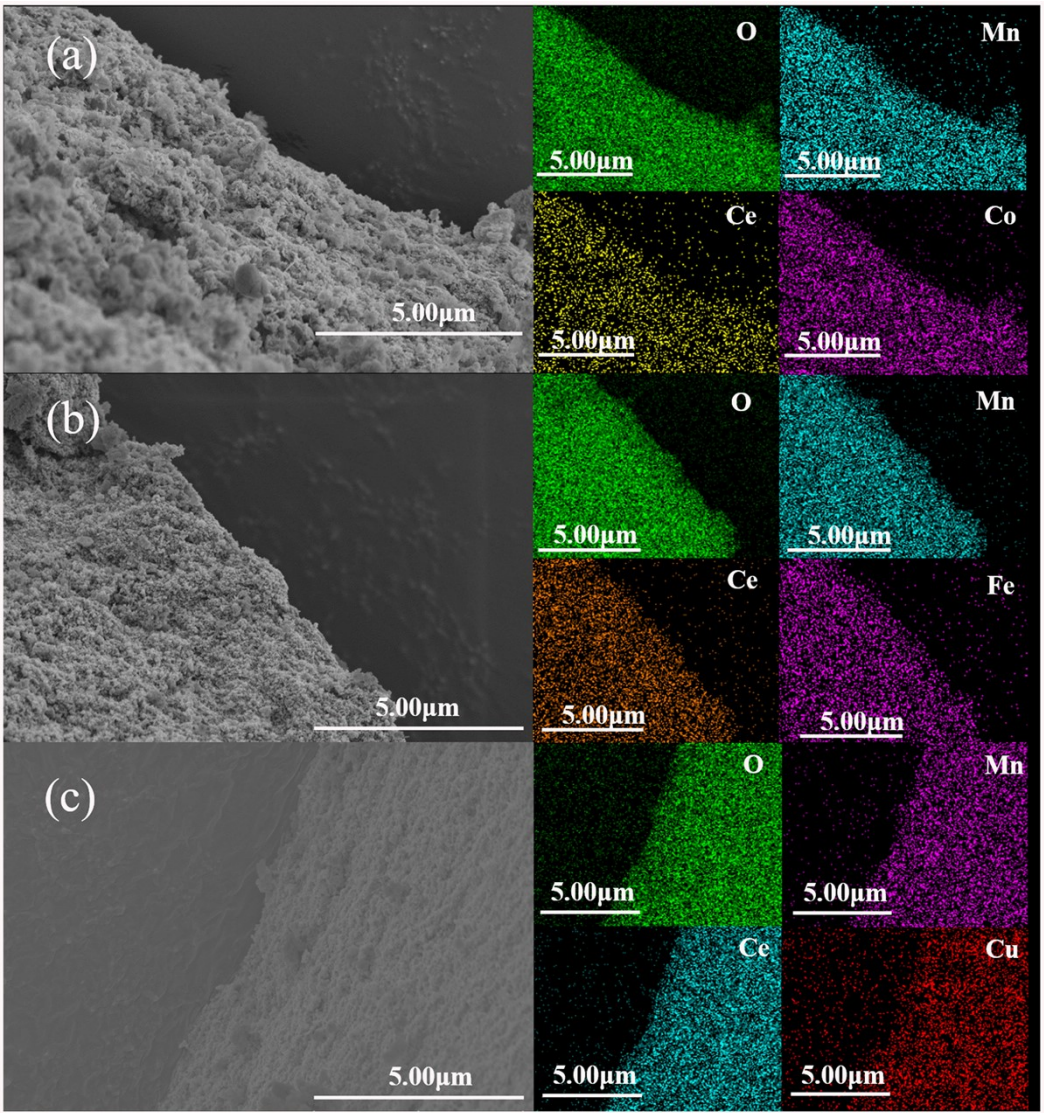

Fig. S10. SEM-EDS analyses of the catalyst samples: (a) Mn-Ce-Co, (b) Mn-Ce-Fe, (c) Mn-Ce-Cu.

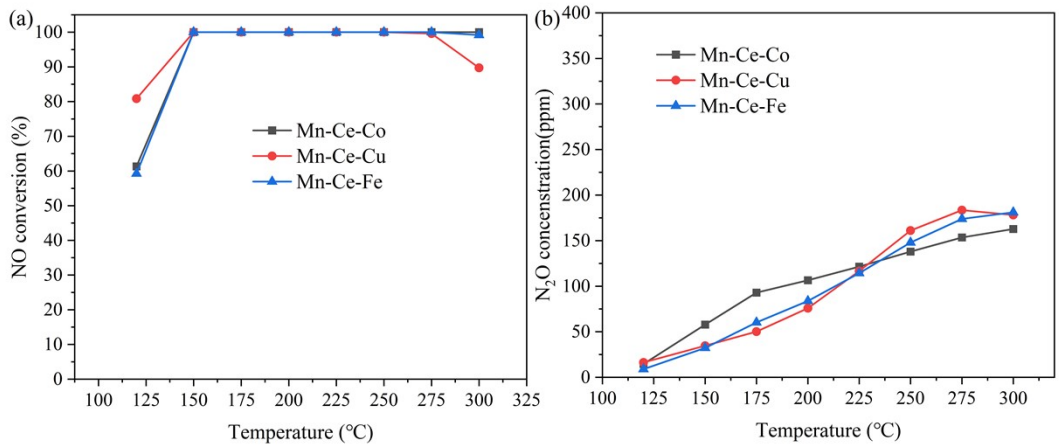

Fig. S11. SCR performance over Mn-Ce-M catalysts (M=Co, Cu, Fe), (a)NO conversion, (b) N_2O yield. Reaction conditions: [NO]=[NH_3]=500ppm, [O_2]=5%, [H_2O]=5%, total flow rate = 200

ml/min, GHSV= 48000 h^{-1}.

Table S1. The features selected for model construction

Pattern	Features	Total number
A	inlet concentration of NO (ppm), NH_3 (ppm), O_2 (%), H_2O (%), GHSV (h^{-1}), catalyst weight (g), specific surface area (m^2/g), mass ratio of the 22 elements	29
B	type, calcination temperature, calcination time, inlet concentration of NO (ppm), O_2 (%), H_2O (%), GHSV (h^{-1}), catalyst weight (g), specific surface area (m^2/g), average pore volume (cm^3/g), molar ratio of the 22 elements	32
C	type, calcination temperature, calcination time, inlet concentration of NO (ppm), O_2 (%), H_2O (%), GHSV (h^{-1}), catalyst weight (g), specific surface area (m^2/g), average pore volume (cm^3/g), molar ratio of the 22 elements	32
D	type, calcination temperature, calcination time, inlet concentration of NO (ppm), O_2 (%), H_2O (%), GHSV (h^{-1}), catalyst weight (g), molar ratio of the 22 elements	30
E	type, calcination temperature, calcination time, inlet concentration of NO (ppm), O_2 (%), H_2O (%), GHSV (h^{-1}), catalyst weight (g), specific surface area (m^2/g), average pore volume (cm^3/g),molar ratio of the 19 elements(Mn, Ti, Ce, O, W, Zr, Ni, Co, Fe, Al, Cu, Si, Sn, Mo, Cr, V, Nb, Mg, Ca)	29

Table S2. The detailed molar ratio of the catalysts

	Abbreviated name in Fig. 6(d)	Formulation	Molar ratio
This work	Co-	Mn-Ce-Co	Mn:Ce:Co=129:18:223
	Cu-	Mn-Ce-Cu	Mn:Ce:Cu=73:69:37
	Fe-	Mn-Ce-Fe	Mn:Ce:Fe=216:47:59
Reference	ref.-1	MnCeCoOx	Mn:Ce:Co=4:5:1
	ref.-2	MnCeCuOx	Mn:Ce:Cu=4:5:1
	ref.-3	MnCeFeOx	Mn:Ce:Fe=4:5:1
	ref.-4	MnCeOx	Mn:Ce=4:6

Table S3. Structural parameters and element content of catalysts

Samples	Structural parameters		
	BET surface area (m^2/g)	Total pore volume (cm^3/g)	Average pore diameter (nm)
Mn-Ce-Co	97.68	0.35	14.94

Mn-Ce-Fe	131.02	0.48	14.14
Mn-Ce-Cu	174.11	0.38	7.65